STRUCTURAL BIOLOGY COMMUNICATIONS

Volume 77 (2021)

Supporting information for article:

Structural insights into the intermolecular interaction of the adhesin SdrC in the pathogenicity of *Staphylococcus aureus*

Junchao Wang, Min Zhang, Mingzhu Wang, Jianye Zang, Xuan Zhang and Tianrong Hang

TABLES:

Table S1. DALI pairwise of SdrC-N2N3 with other members in Clf-Sdr family

	RMSD with SdrC-N2N3
SdrD-N2N3 (4JE0)	2.4 Å
SdrE-N2N3 apo (5WTA)	4.2 Å
SdrG-N2N3 apo (1R19)	2.9 Å
SdrE-N2N3- in CFH peptide complex (5WTB)	3.0 Å
SdrG-N2N3 in Fg peptide complex (1R17)	2.9 Å
ClfA-N2N3-Fg (2VR3)	2.7 Å
ClfB-N2N3-Keratin (4F1Z)	2.3 Å

Structural comparison of SdrC-N2N3 with other Clf-Sdr family proteins through DALI pairwise. The distinctions between different structures were indicated by RMSD (root mean square deviation) value of Cα. All structures were compared using chain A.

FIGURE LEGENDS

Figure S1. **Structural comparison of two SdrC-N2N3 (6LXH and 6LEB) without Ca^{2+}. (a) The position of Mg^{2+} in SdrC-N2N3 (6LEB).** The overall structure of SdrC-N2N3 without Ca^{2+} (6LXH) from Pi et al. (2020). Chain A was colored cyan and orange respectively, while Chain C was colored light gray. N2(N2') and N3(N3') domains in the dimer formed by the two chains were labelled. **(b-d) Superimposition of two SdrC-N2N3 structures (6LXH and 6LEB).** N2N3 domains in our structure (6LEB) were colored green and yellow respectively. Chain A was used in structural comparison. A C-terminal rotation between two structures was labelled, and the obvious differences in structures were indicated by red dashed cycle.

Figure S2. **Structural comparison of SdrC-N2N3 with Ca^{2+} (6LXS) and without Ca^{2+} (6LEB and 6LXH). (a-b) Superimposition of three SdrC-N2N3 structures.** The Ca^{2+} bound structure (6LXS) from Pi et al. (2020) was colored magenta and blue. Other SdrC structures were in colors mentioned in Figure S1. Ca^{2+} in 6LXS was indicated by red arrow, and the major differences in C-terminal tail were cycled. **(c) Comparison of ligand binding site in structures of SdrC-N2N3 and SdrE-N2N3-CFH (PDB: 6LXH and 6LEB).** SdrE-N2N3 in the complex with its ligand peptide CFH (PDB: 5WTB) was colored wheat, and CFH was colored red. The C-terminal β-strand overlapped with CFH peptide in the ligand binding site of Ca^{2+} bound SdrC was indicated by red arrow.

Figure S3. **SDS-PAGE and size-exclusion chromatography (SEC) of SdrC-N2N3 and SdrC-N2 during protein purification. (a) SDS-PAGE of two species of SdrC proteins.** The position of SdrC-N2N3 and SdrC-N2 on SDS-PAGEs were labeled by red box. M, marker; S, supernatant; P, pellet; FT, flow-through; W, wash; E, elution; R, resin. **(b) size-exclusion chromatography of SdrC proteins and measurement of the molecular weights.** Peak 1 and Peak 2 of UV absorption in SEC were indicated as green and yellow respectively, and the relative molecular masses of SdrC proteins were interpolated from the linear regression based on column calibration with standard proteins ferritin (Fer, 440 kDa), aldolase (Ald, 158 kDa), conalbumin (Con, 75 kDa), ovalbumin (Ova, 44 kDa), and chymotrypsin (Chy, 29 kDa). Gel phase distribution coefficients (K_{AV}) were calculated from the respective elution volumes (Ve) and represented as a function of molecular mass.

Figure S4. **SDS-PAGE and size-exclusion chromatography (SEC) of SdrC-N2N3 when His-tag removed from C-terminus by TEV protease. (a) SDS-PAGE of SdrC protein.** The position of SdrC-N2N3 on SDS-PAGE was labeled by red box. M, marker; S, supernatant; P, pellet; FT, flow-through; W, wash; E, elution. **(b) size-exclusion chromatography of SdrC protein.** Peak 1 and Peak 2 of UV absorption in SEC were indicated as green and yellow respectively. The elution volumes (Ve) and their corresponding calculated molecular masses of the peaks were labelled. The TEV protease used for His-tag cleavage had been removed by affinity purification before SEC experiment.

Figure S5. **Interactions on SdrC dimer interface predicted by PDBsum and PDBePISA.** 39 residues from each chain provide 35 potential hydrogen bonds and 298 non-bonded contacts in total (PDBsum). The dimer interface was displayed in two different degree (PDBePISA), and the interaction region was indicated by red dashed cycle.

Figure S6. A model for ligand binding induced SdrC conformational change and dimer breaking. The diagram sketched a hypothetical model for dynamic regulation of SdrC dimer (PDB: 6LEB) upon ligand binding.

Figure S7. The coordination of magnesium ions in SdrC-N2N3 structure. (a) The position of Mg^{2+} in SdrC-N2N3 (6LEB). N2N3 domains in our structure (6LEB) were colored green and yellow respectively, and the interactive molecule (chain B) was shown in light gray. The binding position of Mg^{2+} in structure was indicated by a black dashed box, and six hydrogen-bonds provided by three residues (V288, V232, D230) and three waters to chelate the ion were labelled by black dash. **(b) Superimposition of three SdrC-N2N3 structures.** The Ca^{2+} bound structure (6LXS) from Pi et al. (2020) was colored magenta and blue, SdrC-N2N3 without Ca^{2+} (6LXH) from Pi et al. (2020) was colored cyan and orange, and our structure (6LEB) was colored as above. Chain A was used in structural comparison.

Figure S8. Structures of SdrE-N2N3 apo form and its complex with CFH. (a-b) The overall structures of SdrE-N2N3 (5WTA) and SdrE-N2N3-CFH (5WTB). SdrE-N2N3 (5WTA) was colored lemon green and SdrE-N2N3-CFH (5WTB) was colored wheat with its ligand CFH in red. The C-terminus of SdrE-N2N3 in two structures was labelled. **(c) Superimposition of two SdrE-N2N3 structures.** The differences in C-terminal regions were shown in insets. The electronic map invisible region (587-599) was displayed in apo-formed SdrE-N2N3, and a latch structure found in the complex was labelled by red arrow.

Figure S9. Structures of SdrG-N2N3 and SdrD-N2N3. (a-b) The overall structures of SdrG-N2N3 (1R19) and in the complex with ligand peptide Fibrinogen (1R17). SdrG-N2N3 (1R19) was colored purple and SdrG-N2N3-Fg (1R17) was colored dark gray with Fg in dark green. The C-terminus of SdrG-N2N3 in two structures was labelled. **(c) The overall structures of SdrD-N2N3 (4JDZ).** SdrD-N2N3 (4JDZ) was colored dark yellow, and its C-terminus was labelled.

Figure S10. **Sequence analysis of residues identified by phage display and involved in dimer interface in our SdrC-N2N3 structure.** Two segments, RPGSV (247-251) and VDQYT (288-292) and their corresponding regions in N2 domain were labelled. The residues on dimer interface of SdrC-N2N3 (6LEB) were also highlighted using colors of green and yellow respectively according to their positions in N2-N3 domains. Sequences with region overlapped were indicated by red box.

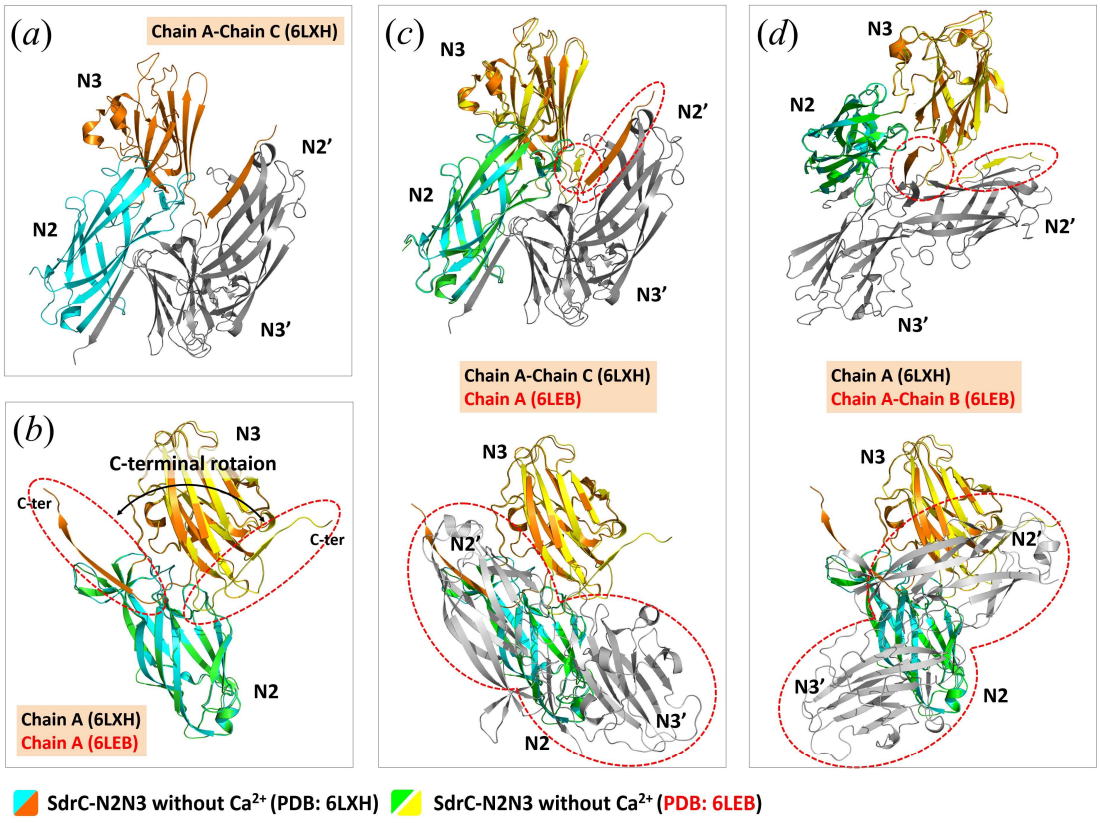
(a)
Chain A-Chain C (6LXH)
N3
N2'
N2
N3'
(b)
N3
C-terminal rotaion
C-ter
C-ter
N2
Chain A (6LXH)
Chain A (6LEB)
(c)
N3
N2'
N2
N3'
Chain A-Chain C (6LXH)
Chain A (6LEB)
N3
N2'
N3'
N2
(d)
N3
N2
N2'
N3'
Chain A (6LXH)
Chain A-Chain B (6LEB)
N3
N2'
N3'
N2
SdrC-N2N3 without Ca2+ (PDB: 6LXH)
SdrC-N2N3 without Ca2+ (PDB: 6LEB)

Figure S1

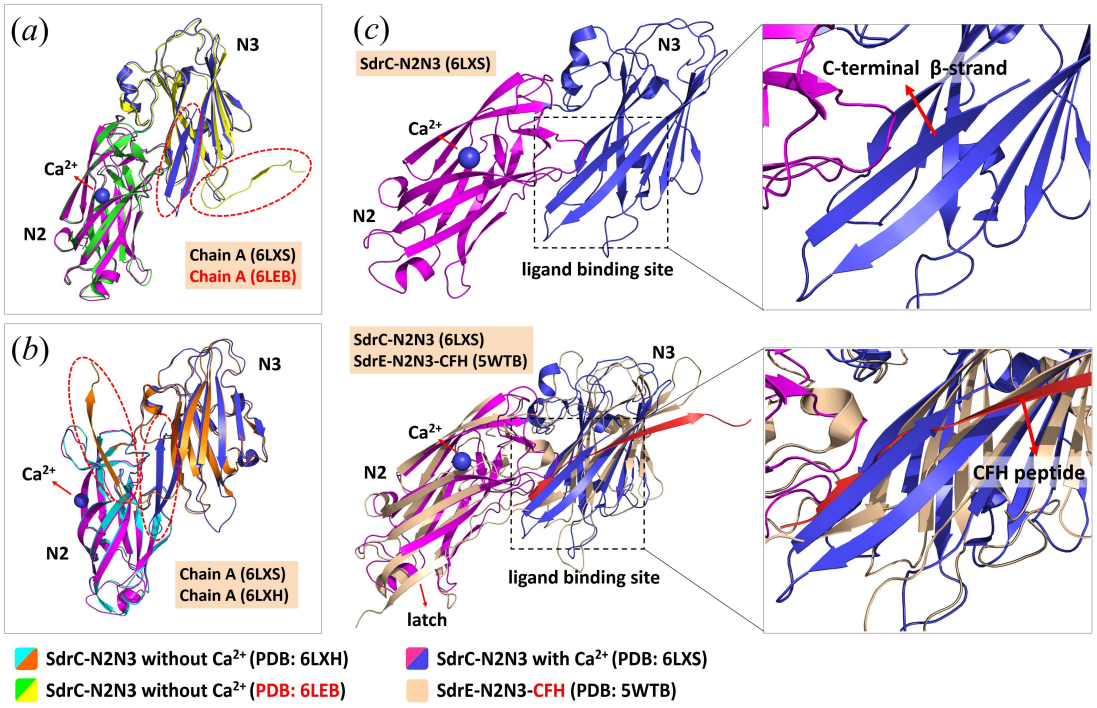
(a)
N3
Ca2+
N2
Chain A (6LXS)
Chain A (6LEB)
(b)
N3
Ca2+
N2
Chain A (6LXS)
Chain A (6LXH)
(c)
SdrC-N2N3 (6LXS)
N3
Ca2+
N2
ligand binding site
C-terminal β-strand
SdrC-N2N3 (6LXS)
SdrE-N2N3-CFH (5WTB)
N3
Ca2+
N2
ligand binding site
latch
CFH peptide
SdrC-N2N3 without Ca2+ (PDB: 6LXH)
SdrC-N2N3 without Ca2+ (PDB: 6LEB)
SdrC-N2N3 with Ca2+ (PDB: 6LXS)
SdrE-N2N3-CFH (PDB: 5WTB)

Figure S2

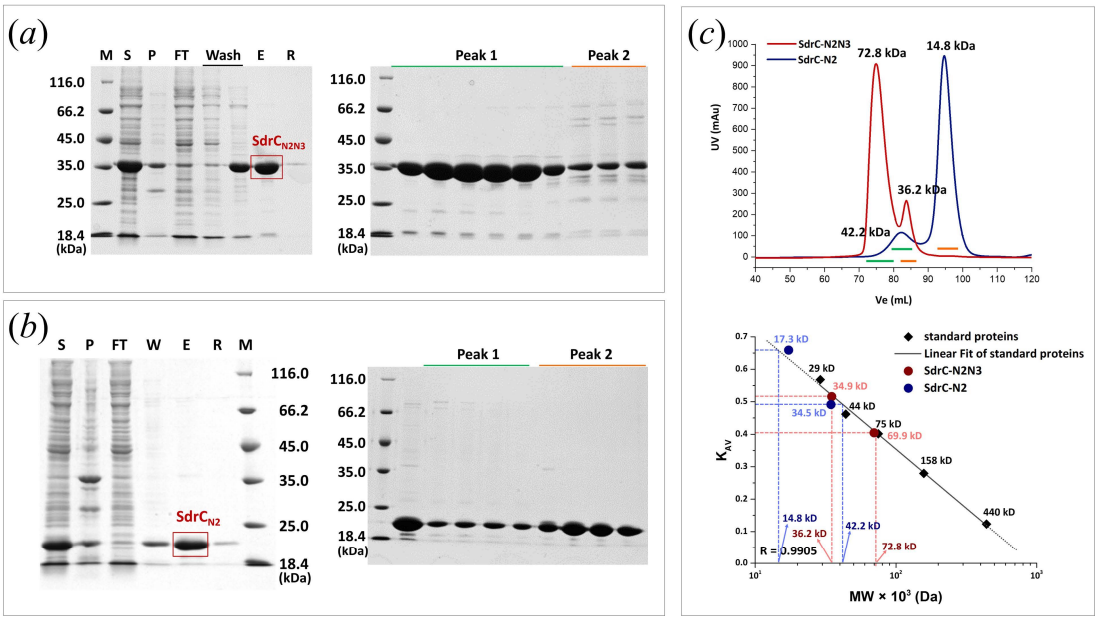
(a)
M S P FT Wash E R
116.0
66.2
45.0
35.0
25.0
18.4
(kDa)
SdrC$_{N2N3}$
Peak 1
Peak 2
(b)
S P FT W E R M
SdrC$_{N2}$
(c)
SdrC-N2N3
SdrC-N2
72.8 kDa
14.8 kDa
36.2 kDa
42.2 kDa
UV (mAu)
Ve (mL)
standard proteins
Linear Fit of standard proteins
SdrC-N2N3
SdrC-N2
17.3 kD
29 kD
34.9 kD
34.5 kD
44 kD
75 kD
69.9 kD
158 kD
440 kD
14.8 kD
36.2 kD
42.2 kD
72.8 kD
R = 0.9905
K_{AV}
MW × 10^3 (Da)

Figure S3

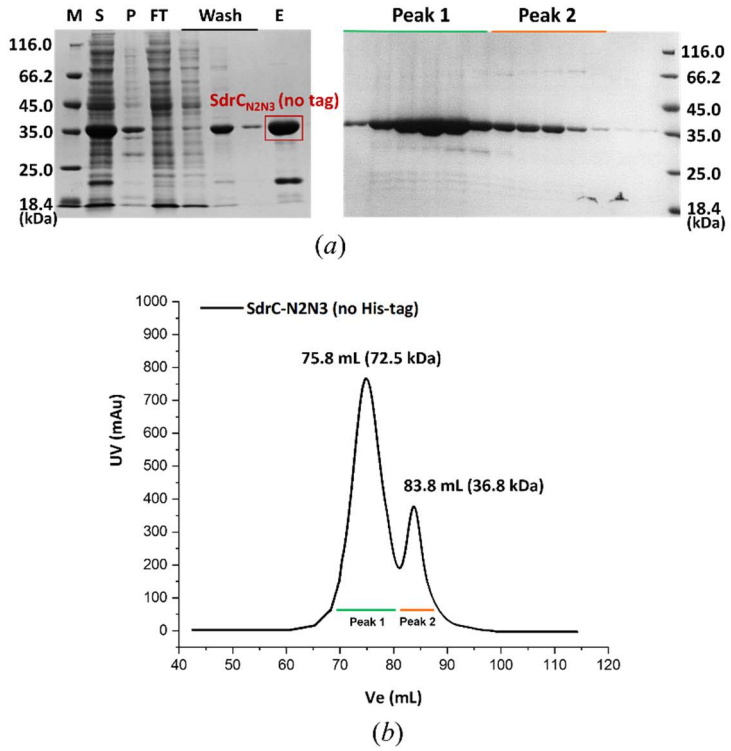
M S P FT Wash E
Peak 1 Peak 2
116.0
66.2
45.0
35.0
25.0
18.4
(kDa)
SdrC$_{N2N3}$ (no tag)
(a)
SdrC-N2N3 (no His-tag)
75.8 mL (72.5 kDa)
83.8 mL (36.8 kDa)
Peak 1
Peak 2
UV (mAu)
Ve (mL)
(b)

Figure S4

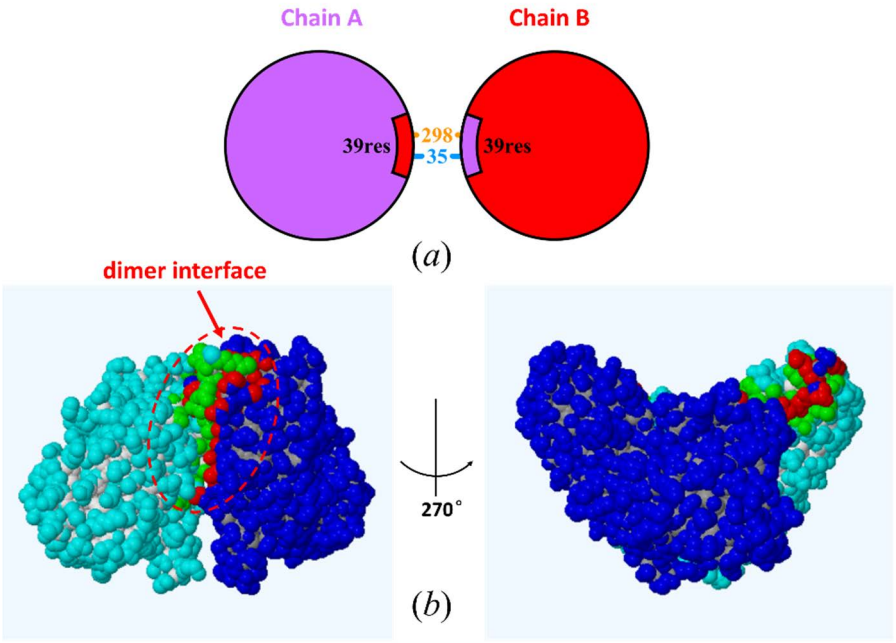

Figure S5

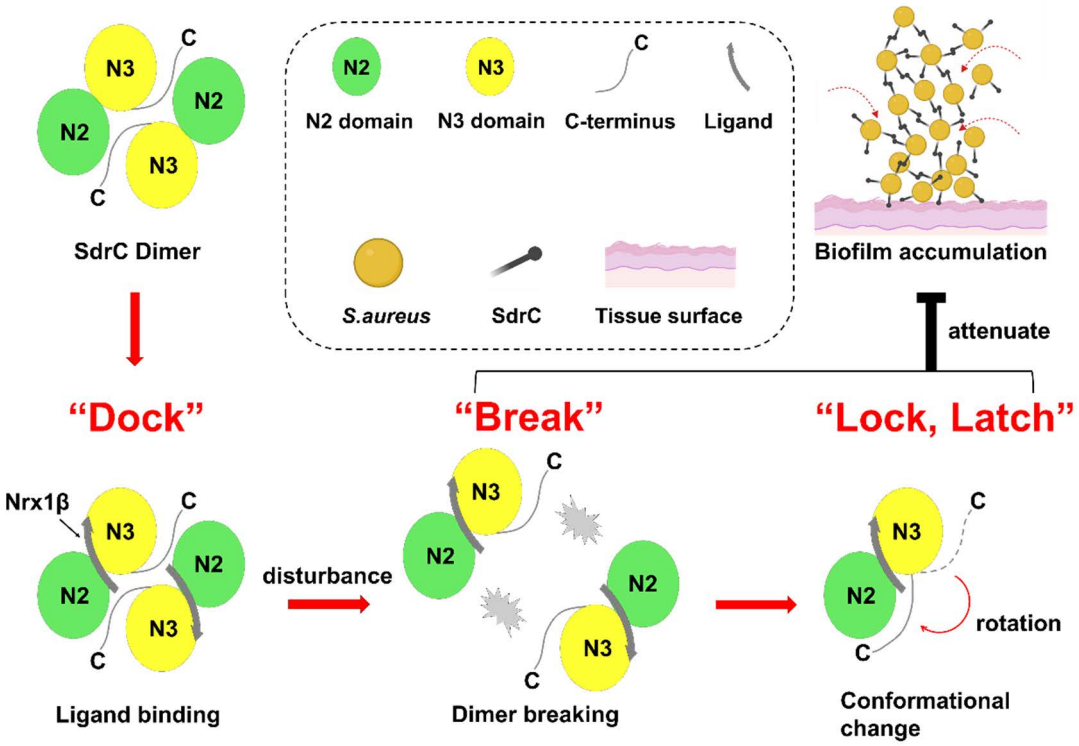
N3
N2
N2
N3
C
C
SdrC Dimer
N2
N3
C
N2 domain
N3 domain
C-terminus
Ligand
S.aureus
SdrC
Tissue surface
Biofilm accumulation
attenuate
"Dock"
"Break"
"Lock, Latch"
Nrx1β
Ligand binding
disturbance
Dimer breaking
rotation
Conformational change

Figure S6

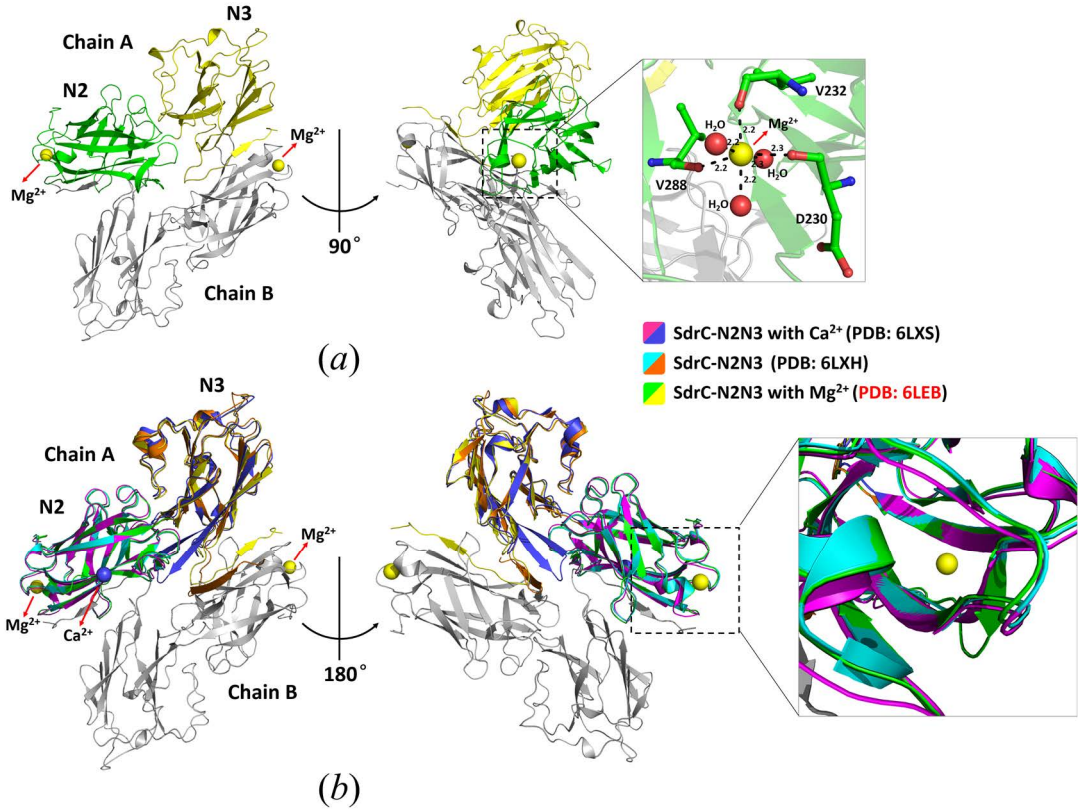
N3
Chain A
N2
Mg2+
Mg2+
90°
Chain B
V232
H2O
Mg2+
V288
H2O
D230
(a)
SdrC-N2N3 with Ca2+ (PDB: 6LXS)
SdrC-N2N3 (PDB: 6LXH)
SdrC-N2N3 with Mg2+ (PDB: 6LEB)
N3
Chain A
N2
Mg2+
Mg2+
Ca2+
180°
Chain B
(b)

Figure S7

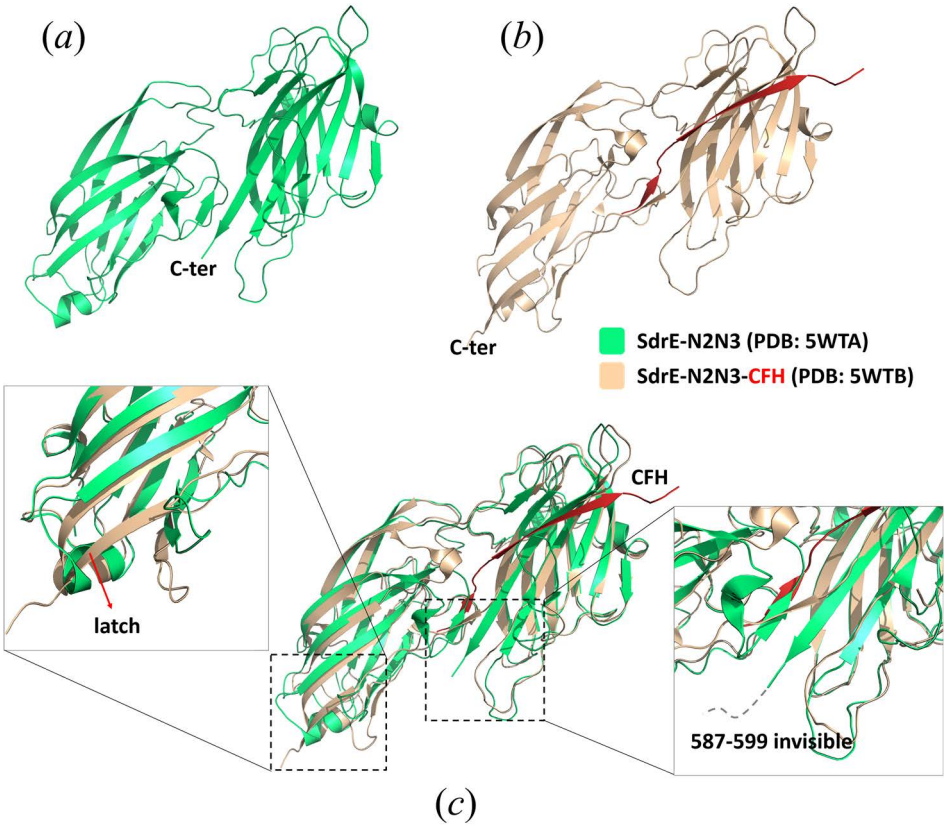
(a)
C-ter
(b)
C-ter
SdrE-N2N3 (PDB: 5WTA)
SdrE-N2N3-CFH (PDB: 5WTB)
latch
CFH
587-599 invisible
(c)

Figure S8

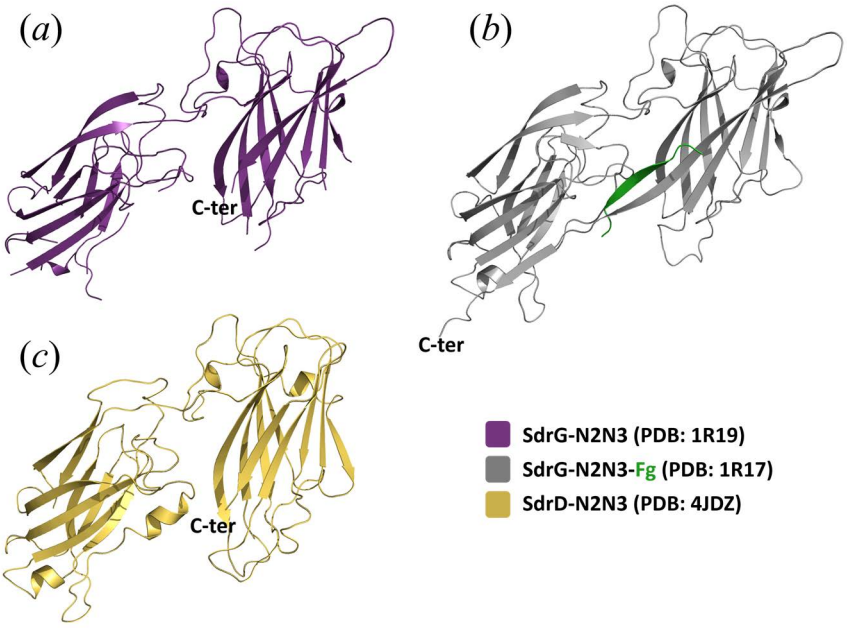
(a)
C-ter
(b)
C-ter
(c)
C-ter
SdrG-N2N3 (PDB: 1R19)
SdrG-N2N3-Fg (PDB: 1R17)
SdrD-N2N3 (PDB: 4JDZ)

Figure S9

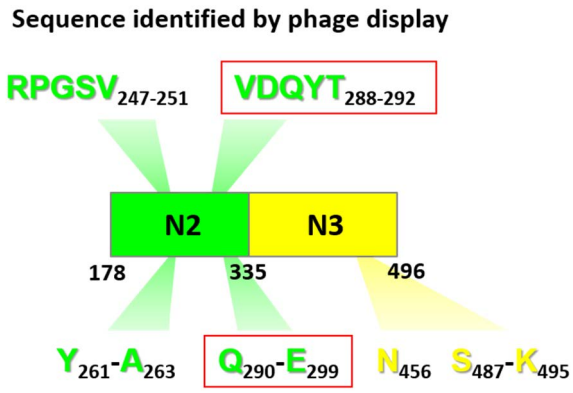
Sequence identified by phage display
RPGSV247-251
VDQYT288-292
N2
N3
178
335
496
Y261-A263
Q290-E299
N456
S487-K495
Sequence on dimer interface (PDB: 6LEB)

Figure S10